HEAT-TOLERANT FLEXIBLE CHALCOPYRITE SOLAR CELLS VIA ALL-SPUTTERED CD-FREE ELECTRON TRANSPORT LAYERS

Hiroki Sugimoto[1], Kazuhito Fukasawa[1], Mayo Kawahara[1], Yoshiaki Hirai[1], and Akira Yamada[2]

[1]PXP Corporation, Nishihashimoto, Sagamihara, Kanagawa, Japan
[2]Tokyo Institute of Technology, Ookayama, Meguro-ku, Tokyo, Japan

Hiroki.Sugimoto@pxpco.jp

ABSTRACT: Heat-tolerant flexible chalcopyrite Cu(In, Ga)(Se, S)$_2$ (CIGSS) solar cells were realized by introducing all-sputtered Cd-free electron transport layers (ETLs). The samples with the newly developed double ETLs showed no degradation after a long-time super heat acceleration test under the light soaking, while the samples with conventional ETLs showed large degradation. Especially fill factor drop was completely restricted, which was considered to be ascribed to the barrier effects of the new ETLs against the alkaline diffusion from the CIGSS absorber to the transparent conductive oxide through the ETLs. These results contribute to the installation of the CIGSS solar cells into the relatively higher temperature environments than the conventional ground-mounted solar cells, such as the rooftop of vehicles and the space satellites. In addition, the all-sputtered ETLs will reduce the production cost of the CIGSS solar cells due to the elimination of the high-cost conventional manufacturing processes for the ETL deposition, such as the chemical bath deposition, the chemical vapor deposition and the atomic layer deposition.
Keywords: Chalcopyrite, Cu(In, Ga)(Se, S)$_2$, CIGSS, Cd-free, All-sputter

1 INTRODUCTION

Recently, light-weight and flexible solar cells have attracted a lot of attention for the application in vehicles, drones and space satellites as well as buildings. PXP corporation (one of the small start-up company in Japan) has been developing low cost, extra light and flexible, high durability and high performance solar cells, aiming to expand thin-film photovoltaic (PV) applications into new fields, such as building integrated PV (BIPV), vehicle integrated PV (VIPV) and aerospace applications. In order to develop the next-generation solar cells applicable to these new fields, the study on durability against the higher temperature than the conventional ground-mounted PV applications is very important, because the solar cells under the anormal environments, such as the rooftop of the vehicles and the space satellites, sometimes shows much higher temperature than the ground-mounted solar cells. In these fields, the long-time heat tolerance against the temperature above 100C and up to 150C is sometimes required.

So far, a lot of papers have reported the heat stability on the chalcopyrite solar cells. According to the comprehensive review for stability tests on the chalcopyrite solar cells, the interactions among the transparent conductive oxide (TCO), the electron transport layer (ETL) and the chalcopyrite absorber were the most important key to determine the heat tolerance [1]. However, most of these papers were related to the conventional stability test around the temperature of 85C, which described that tea chalcopyrite solar cells had good heat tolerance and there was no significant difference in the degradation ratio among the variety of ETLs [2, 3]. The other papers reported the impact of the high temperature treatment above 200C within a short time (from 15min to 60min) against the variety of ETLs, such as conventional CdS [4], Cd-free In_2S_3 [5], ZnOS [6] and ZnMgO [7]. They concluded the intermixture between the ETLs and the absorbers caused degradations of the cell parameters. Not only the intermixture, but also the Na diffusion from the absorber to the TCO through the ETL was also reported to be related to the degradations [8]. Especially, the Na diffusion is considered to be the dominant factor of the degradation at the temperature range from 100C to 200C due to the low migration energy of the Na atoms in the chalcopyrite absorbers (the migration energy just about 0.3eV) [9]. There are a few reports for the investigation of the long-time heat tolerance at the temperature range from 100C to 200C [10,11]. So far, it has been difficult to prevent the Na-related degradation by the long-time heat exposure above 100C.

The purpose of this paper is to establish the heat-tolerant (up to 150C) flexible chalcopyrite Cu(In, Ga)(Se, S)$_2$ (CIGSS) solar cells by applying new ETLs. In addition, taking into account the future mass-production, we also developed the all-sputtered Cd-free ETLs, in order to reduce the production cost of the CIGSS solar cells by eliminating the high-cost conventional ETL processes, such as the chemical bath deposition (CBD), the chemical vapor deposition and the atomic layer deposition (ALD). The conventional ETL deposition method is the wet process, however it is inconvenient because both the absorber fabrication process and the TCO deposition process are the dry process. The cost impact of the introduction of all-dry ETL should be very big because it can eliminate useless repetition of vacuum brake and vacuum back as well as a plenty of toxic waste disposal.

2 EXPERIMENTAL DETAILS

In order to investigate the heat tolerance, the flexible CIGSS solar cells with the variety of ETLs were prepared. The CIGSS solar cells used for this study were specially developed for the severe space environments. Not only the high temperature tolerance but also the radiation hardness, the thermal cycle tolerance and the mechanical vibration tolerance were much improved than the conventional CIGSS solar cells [12]. The CIGSS solar cells were fabricated by highly productive sputtering-based process. The basic structure was Ag grid electrode/In_2O_3:H (IOH) TCO/ETLs/CIGSS absorber/Mo back electrode on flexible Ti film. In this study, anti-reflective (AR) coating was not deposited, however, normally relative efficiency (Eff) gain of around 8% by the AR coating has been confirmed for our cells. The thickness of the CIGSS device layer and the Ti substrate was about 3 um and 50 um, respectively. The weight of our standard CIGSS solar cells were about 250 g/m^2 (minimally 150 g/m^2 achievable).

Regarding the ETLs, at first, the conventional CdS cells with the ETL thickness of 75 nm were fabricated by the CBD method. Then, we introduced the sputtered $ZnTiO_x$ layer as the secondary wide-gap ETL on the CdS layer. The thickness of optimized $ZnTiO_x$/CdS double ETLs was 70nm and 30nm, respectively. Note that the initial efficiency (Eff) and the heat tolerance of the CdS cells and the $ZnTiO_x$/CdS cells were similar, thus the results of only the $ZnTiO_x$/CdS cells were shown in this paper. We also developed the Cd-free cells by introducing $ZnTiO_x$ single ETL with the thickness of 100nm. Finally, all-sputtered Cd-free $ZnTiO_x$/In_2S_3 double ETLs were developed as the heat tolerant and highly productive ETLs. The thickness of optimized $ZnTiO_x$/In_2S_3 double ETLs was 70nm and 30nm, respectively.

After the cell fabrication, all samples were pre-stabilized by the light soaking (LS) at 200C30min in N_2 box in order to eliminate over estimation of improvement effects by the LS. After the initial measurement of the electrical parameters, the super heat acceleration test (SHT) was performed at 150C208h under the LS in N_2 box. Then, the heat effect in dark was investigated at 150C65h in dark N_2 box. Finally, recovery effect by the LS was also investigated at 150C44h under the LS in N_2 box. The changes in the electrical parameters at respective steps were also measured.

The current–voltage (J-V) characteristics were measured by a class A solar simulator (XI-05A1V2-L, SERIC Ltd., Japan) with AM 1.5 and 100 mW/cm^2 illumination at room temperature. External quantum efficiency (EQE) curves ranging from wavelength of 300 nm to 1300 nm were measured by a spectral response measurement system (CEP25-MLT, Bunkoukeiki Co., Ltd., Japan) at room temperature without any bias. The bandgap of the CIGSS cells were extracted from the EQE curves with the derivative method [13]. Then, open circuit voltage (V_{oc}) deficit was calculated with the bandgap and V_{oc}.

3 RESULTS AND DISCUSSION

Figures 1(a)-(c) show the schematic images of the long-time SHT condition and device structures with the variety of ETLs, such as the $ZnTiO_x$/CdS double ETLs, the $ZnTiO_x$ ETL, and the $ZnTiO_x$/In_2S_3 double ETLs. The CdS layer was deposited by the CBD and the $ZnTiO_x$ layer and the In_2S_3 layer were deposited by sputtering. Before the SHT, devices were pre-stabilized by the LS at 200C30min in order to eliminate over estimation of improvement effects by the LS, then the SHT was performed at 150C208h under the LS in N_2 box.

The J-V characteristics of the $ZnTiO_x$/CdS cell, the $ZnTiO_x$ cell, and the $ZnTiO_x$/In_2S_3 cell before and after the SHT are shown in Figs 1(d)-(f). The $ZnTiO_x$/In_2S_3 double ETL cell showed no degradation after the SHT, while the $ZnTiO_x$/CdS double ETL cell and the $ZnTiO_x$ ETL cell showed large degradation. The degradation mainly caused by the fill factor (FF) drop, while the V_{oc} and the short circuit current (J_{sc}) were stable. We confirmed the conventional CdS ETL cell also showed the FF drop as same as the $ZnTiO_x$/CdS double ETL cell and the $ZnTiO_x$ ETL cell. On the other hand, the FF drop was completely restricted by the $ZnTiO_x$/In_2S_3 double ETL cell. From these results, we concluded that the important key for preventing the heat degradation should be the insertion of the In_2S_3 layer. The type of the deposition method was seemed to be less impact against the heat degradation. We also tried the In_2S_3 single ETL cell, however the initial V_{oc}

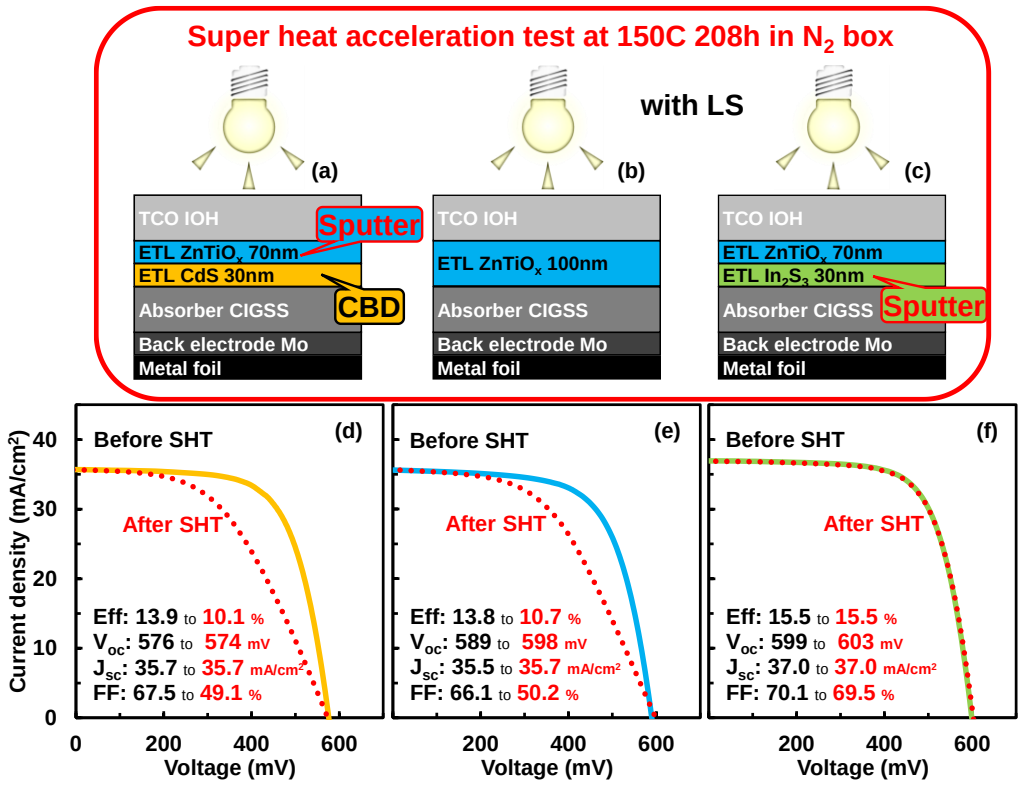

Figure 1: Schematic images of long-time SHT condition and device structures with a variety of ETLs, (a) $ZnTiO_x$/CdS double ETLs, (b) $ZnTiO_x$ ETL, and (c) $ZnTiO_x$/In_2S_3 double ETLs. CdS layer was deposited by CBD and $ZnTiO_x$ layer and In_2S_3 layer were deposited by sputtering. J-V characteristics of (a) $ZnTiO_x$/CdS cell, (b) $ZnTiO_x$ cell, and (c) $ZnTiO_x$/In_2S_3 cell before (solid lines) and after (dashed lines) SHT.

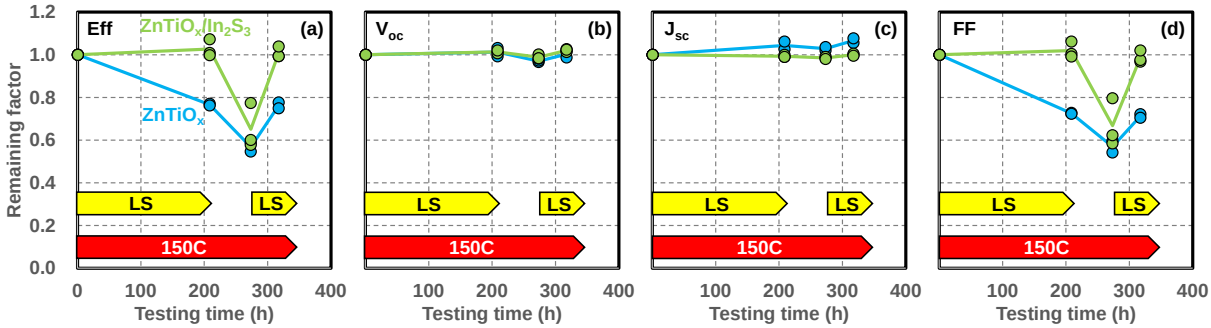

Figure 2: Changes in remaining factor of (a) Eff, (b) V_{oc}, (c) J_{sc}, and (d) FF on $ZnTiO_x$ cells (blue) and (c) $ZnTiO_x/In_2S_3$ cells (green) by SHT under LS at 150C208h, SHT in dark at 150C65h, and SHT under LS at 150C44h. Solid lines show the averaged remaining factors of respective cells.

degradation caused by the deposition damage of the TCO sputtering was not prevented. Introducing thicker In_2S_3 single ETL was one of the ways to prevent the TCO sputtering damages, however initial J_{sc} was decreased due to the less light transmission in the short wavelength region by the low bandgap of In_2S_3. This was why we introduced the wide-gap $ZnTiO_x$ layer on the In_2S_3 layer. Then we compared the ALD and the sputtering for the deposition technique of the $ZnTiO_x$. After optimization of deposition condition, fortunately the sputtered $ZnTiO_x$ cells showed comparable initial Eff with the ALD deposited $ZnTiO_x$ cells. Thus, the all-sputtered Cd-free $ZnTiO_x/In_2S_3$ double ETL structure was introduced as our basic cell structure. The strong heat tolerance of In_2S_3 layer was considered to be ascribed to the barrier effects of the ETLs against the Na diffusion from the CIGSS absorber to the TCO through the ETLs.

Figure 2 shows the changes in remaining factor of each electrical parameter on the $ZnTiO_x$ cells and the $ZnTiO_x/In_2S_3$ cells. Before the SHT, devices were also pre-stabilized by the LS at 200C30min in order to eliminate over estimation of improvement effects by the LS. At first, the SHT was performed at 150C208h under the LS in N_2 box, then in order to investigate the dark heat effects, samples were heated at 150C65h in dark N_2 box. Finally, the LS was applied again at 150C44h in N_2 box for checking the recovery effects by the LS. As same as the results shown in Fig 1(e) and (f), the $ZnTiO_x/In_2S_3$ cells also showed no degradation after the first SHT also in Fig. 2, while the $ZnTiO_x$ cells showed large degradation due to the FF drop. In this experiment, the $ZnTiO_x$ cells showed slight J_{sc} increasement. This was considered to be due to the widening of the space charge region by the decrease in the carrier density of the CIGSS absorber. We believe the alkaline diffusion in the $ZnTiO_x$ cells should decrease the carrier density. Then, after the dark heat at 150C65h, both the $ZnTiO_x/In_2S_3$ cells and the $ZnTiO_x$ cells showed the FF drop, however the FF drop was completely recovered by the successive LS at 150C44h. We considered these phenomena caused by the metastable behavior of the defect complex of Cu-vacancies and Se-vacancies (V_{Cu}-V_{Se}). The V_{Cu}-V_{Se} defects initially act as the donor-like defects, then they turn into the acceptor-like defects by the LS. However, they easily turn back to the initial state by the successive dark heating. We believe the temporary FF drop was caused by the decrease in the carrier density due to the changes in the electrical state of the V_{Cu}-V_{Se} defects by the dark heat.

Then, optimization of the Cd-free double ETLs was performed. Figure 3(a) shows the V_{oc} deficit of the $ZnTiO_x$/CdS cells, the $ZnTiO_x$ cells, and the $ZnTiO_x/In_2S_3$ cells. We confirmed not only the heat-tolerance but also the V_{oc} deficit was improved by the $ZnTiO_x/In_2S_3$ double ETLs as compared with the conventional ETLs. Finally, Eff of 16.9% was achieve by the all-sputtered Cd-free $ZnTiO_x/In_2S_3$ cell without AR coating, as shown in Fig 3(b). These results contribute to the installation of the CIGSS solar cells in the relatively higher temperature environments than the conventional ground-mounted solar cells, such as the rooftop of vehicles and the space satellites. In addition, these achievements will reduce the production cost of the CIGSS solar cells due to eliminating the high-cost conventional manufacturing processes for the ETL depositions.

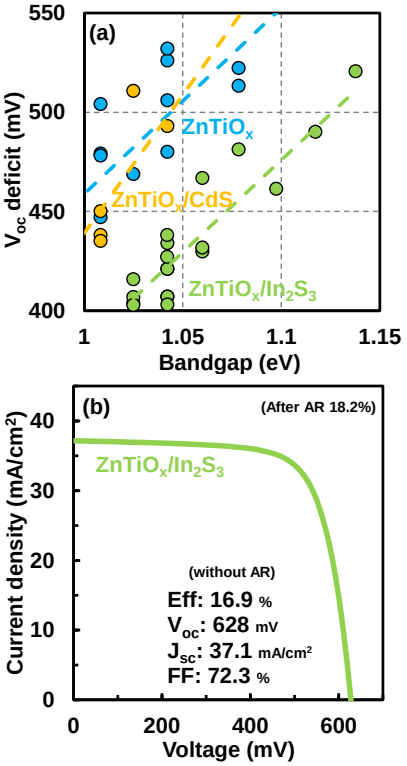

Figure 3: (a) V_{oc} deficit of $ZnTiO_x$/CdS cells (orange), $ZnTiO_x$ cells (blue), and $ZnTiO_x/In_2S_3$ cells (green). Dashed lines show fitted lines of respective cells. (b) J-V characteristics of optimized. $ZnTiO_x/In_2S_3$ cell without AR coating.

4 SUMMARY

In this paper, we investigated the durability against the higher temperature than the conventional ground-mounted PV applications. At first, we prepared test samples with variety of ETLs and performed SHT at 150C208h in N_2 box with the LS. The samples with the $ZnTiO_x/In_2S_3$ double ETLs showed no degradation after the SHT, while the samples with conventional ETLs showed large degradation. We also investigated the heat effects in dark, then temporary FF drop was observed, however it was fully recovered after the LS. After optimization of ETLs, we confirmed not only the heat-tolerance but also the V_{oc} deficit was improved by the newly developed double ETLs as compared with the conventional ETLs. Finally, the Eff of 16.9% without the AR coating was achieved by the all-sputtered Cd-free $ZnTiO_x/In_2S_3$ double ETLs. We believe these results will contribute to the expansion of the thin-film PV into the BIPV, VIPV and aerospace applications.

REFERENCES

[1] M. Theelen, and F. Daume, Solar Energy, vol. 133 (2016) 586.

[2] N.A. Allsop, A. Hänsel, S. Visbeck, T.P. Niesen, M.C. Lux-Steiner, and Ch.-H. Fischer, Thin Solid Films, vol. 511 (2006) 55.

[3] S. Spiering, D. Hariskos, S. Schröder, and M. Powalla, Thin Solid Films, vol. 480 (2005) 195.

[4] A. Koprek, P. Zabierowski, M. Pawlowski, L. Sharma, C. Freysoldt, B. Gault, R. Wuerz, and O. Cojocaru-Mir´edin, Solar Energy Materials and Solar Cells, vol. 224 (2021) 110989.

[5] N. Naghavi, J.-F. Guillemoles, D. Lincot, B. Canava, A. Etcheberry, S. Taunier, S. Spiering, M. Powalla, M. Lamirand, and L. Legras, Proceedings 19th European Photovoltaic Solar Energy Conference (2004) 1733.

[6] J-H. Wi, T. G. Kim, J. W. Kim, W-J. Lee, D-H. Cho, W. S. Han, and Y-D. Chung, ACS Applied Materials and Interfaces, vol. 7 (2015) 17425.

[7] C-S. Lee, S. Kim, E. A. Al-Ammar, HS Kwon, and B. T. Ahn, ECS Journal of Solid State Science and Technology, vol. 3 (2014) Q99.

[8] H. A. Yetkin, T. Kodalle, T. Bertram, A. Villanueva-Tovar, M. Rusu, R. Klenk, B. Szyszka, R. Schlatmann, and C. A. Kaufmann, Progress in Photovoltaics, vol. 29 (2021) 1034.

[9] T. Maeda, A. Kawabata, and T. Wada, Japanese Journal of Applied Physics, vol. 54 (2015) 08KC20.

[10] M. Theelen, V. Hans, N. Barreau, H. Steijvers, Z. Vroon, and M. Zeman, Progress in Photovoltaics, vol. 23 (2015) 537.

[11] T. Ott, T. Walter, D. Hariskos, O. Kiowski, and R. Schaffler, IEEE Journal of Photovoltaics, vol. 3 (2013) 514.

[12] H. Sugimoto, T. Nakamura, M. Imaizumi, S. Sato, and T. Ohshima, Proceedings 50th IEEE Photovoltaic Specialist Conference (2023) unpublished.

[13] R. Carron, C. Andres, E. Avancini, T. Feurer, S. Nishiwaki, S. Pisoni, F. Fu, M. Lingg, Y. E. Romanyuk, S. Buecheler, and A. N. Tiwari, Thin Solid Films, vol. 669 (2019) 482.